Development of a metrological scanning probe microscope as a primary standard for nanoscale dimensional measurement

B. Babic, C. Freund, M. B. Gray, J. Herrmann*, M. T. L. Hsu, M. Lawn and T. G. McRae

National Measurement Institute Australia, Lindfield NSW 2070, Australia
*Corresponding author: Email: jan.herrmann@measurement.gov.au

ABSTRACT

We present an overview of the design of the metrological scanning probe microscope (mSPM) currently under development at the National Measurement Institute Australia (NMIA) and report on preliminary results on the characterization of key components. The mSPM is developed as part of the nanometrology program at NMIA and will provide dimensional measurements made at the nanometer scale that are traceable to the realization of the SI meter at NMIA. The design of the mSPM follows metrological principles to achieve accurate position measurement, over an addressable measurement volume of 100 µm × 100 µm × 25 µm, with a target combined uncertainty of 1 nm. It minimizes uncertainty contributions from deformation of the frame, alignment errors and effects of environmental fluctuations. It incorporates a quartz tuning fork (QTF) detector and a high-performance heterodyne laser interferometrysystem.

Keywords***: metrology; nanoscale; AFM; non-contact mode; quartz tuning fork; laser interferometry***

1 INTRODUCTION

The capability for accurate dimensional measurement at the nanoscale, traceable to the SI meter, is fundamental for the development and effective support of nanoscience and nanotechnology. At the National Measurement Institute Australia (NMIA), the primary standard for dimensional measurement at the nanoscale is being realized with a metrological scanning probe microscope (mSPM). NMIA's SPM metrology laboratory links dimensional measurements at the nanometer scale with the realization of the SI meter at NMIA. The key element of this link is an mSPM which combines the nanometer scale precision of dimensional measurements achievable with SPM with the accuracy and traceability achievable with laser interferometry.

Here, we present an overview of the design and operation of the mSPM, highlight the features specifically associated with an instrument based on a quartz tuning fork detector, describe the high-performance laser interferometry system developed for the mSPM and present characterization results for some of the instrument's key components.

2 INSTRUMENT COMPONENTS AND DESIGN PRINCIPLES

Experience in designing ultra-high precision mechanical stages and instruments [1] and in operating similar mSPMs at other metrology institutes [2–5] has shown that there are many potential contributions to the uncertainty of the position measurements. These include alignment errors (particularly Abbé errors [6]); deformations of the mechanical structures (for instance due to thermal expansion); motion errors of the translation stage; form errors of the interferometer mirrors; nonlinearities of the interferometers; and fluctuations in the refractive index of air.

NMIA's mSPM design aims to minimize the magnitude of the contributions to the total uncertainty. For example, to minimize the Abbé offsets and associated errors, the probe tip is fixed with respect to the metrological frame, and the interferometers are aligned such that their beams virtually intersect at the tip.

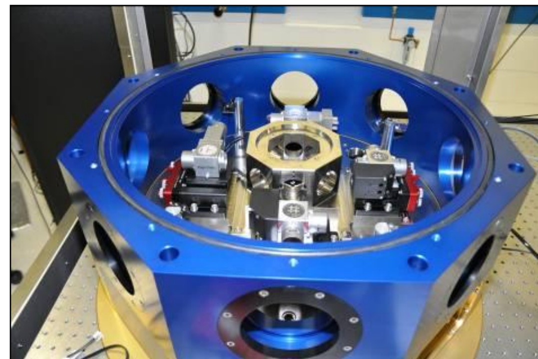

Figure 1: Photograph of NMIA's mSPM showing the metrological frame, some of the laser interferometers, parts of the beam delivery system and parts of the environmental enclosure.

The metrological frame is designed as an octagonal prism symmetric around a vertical axis that runs through the SPM probe tip (Figure 1). Where possible, components are kinematically mounted to minimize distortions due to thermal expansion, and the rigid structure of the metrological frame aims to reduce the effects of ambient vibrations. To minimize the metrological loop, no coarse stages are used for sample positioning. The sample is

scanned with respect to the fixed tip by means of a three-axis piezo-actuated flexure translation stage. The stage motion is measured by five laser interferometers, one for each translation axis and two to monitor rotations (yaw, pitch and roll).

2.1 Sample Translation Stage

Translation stages are commercially available for research grade SPMs, optical microscopy, lithography, optical fiber alignment and other applications requiring sub-nanometre resolution positioning. A translation stage with an XY-axes scan range of 100 µm × 100 µm and a range in the Z-axis of 25 µm has been selected for the NMIA mSPM. The stage features a 25 mm aperture along the Z-axis for optical access.

The translation stage consists of a central moving platform linked to a static base with flexure hinges which guide the motion by deformation of the flexure material, thereby allowing smooth friction and stiction-free motion. The translation stage has the capability of closed-loop operation, whereby the position of the moving platform is monitored by either capacitive sensors incorporated into the stage, or by external sensors such as interferometers. This allows the controller to correct for positioning errors by adjusting the voltages applied to the actuators. The mSPM design also incorporates interferometers arranged opposite the X-axis and Y-axis linear displacement interferometers to measure the angular stage errors.

The requirement to implement closed-loop control of the tip-sample interaction based on the motion of the translation stage places significant design constraints on the mSPM. The mechanical resonance frequencies of the translation stage for motion along the X-, Y-, and Z-axes have been measured. The frequency responses of the nanopositioning stage for motion along the three axes are shown in Figure 2. The values of the fundamental resonance frequencies are 308 Hz, 321 Hz and 805 Hz, for the X-, Y-, and Z-axes, respectivly.

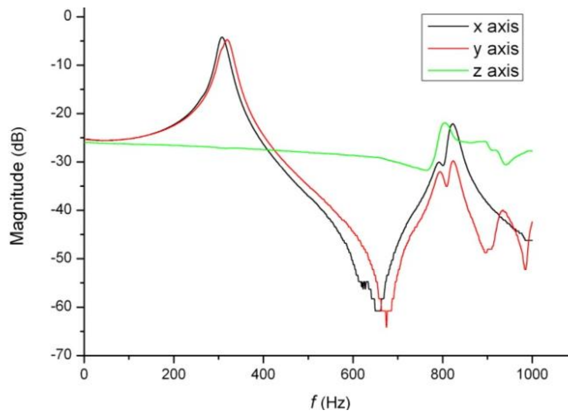

Figure 2. Frequency responses of the unloaded nano-positioning stage for each of the axes (X,Y,Z). Excitation: sinusoidal, 10 mV peak-to-peak.

The resonance frequencies of the unloaded nanopositioning stage are reduced by the additional mass of the mirror assembly and the sample stage. For the *X*- and *Y*-axes, we have measured a reduction in the resonance frequencies of approximately 25 %, while for the *Z*-axis the resonance frequency is reduced by 40 %. Our experience has shown that these operational resonance frequencies allow reliable imaging at a scan rate of 1 Hz and a resolution of 512 points per scan line.

2.2 Interferometry

The mSPM displacements were measured using plane mirror differential laser interferometers. A synthetic heterodyne laser source, whereby the heterodyne frequency was tunable by up to 10 MHz, was implemented. This source has superior polarization orthogonality (by up to 60 dB) that therefore minimizes cyclic error arising from polarization cross-coupling. The source was also frequency stabilized to a Zeeman-split HeNe laser within 2 parts in 10^9, to provide absolute frequency stability and traceability to the SI definition of the metre. The measured contribution of the cyclical error of the interferometry system to the displacement measurement is of the order of 100 pm [7]. The phase is measured using an all-digital phase meter based on a phase locked loop (PLL) and implemented on a field programmable gate array, with >70 dB common mode rejection and sub-µrad $Hz^{-1/2}$ phase noise [8]. The interferometer's displacement sensitivity is 1 pm $Hz^{-1/2}$ above ~5 Hz and 0.1 pm $Hz^{-1/2}$ above ~50 Hz. Integration of the interferometric displacement measurement with the AFM control system allows performing dimensional measurements that are traceable to the SI metre.

2.3 Quartz Tuning Fork Detector

The mSPM operates in non-contact frequency modulation (FM) dynamic atomic force microscopy (AFM) mode [9], with a tip mounted on a tine of a piezoelectric quartz tuning fork (QTF) acting as the force sensor. The QTF is driven electrically at a resonance. The shift of the QTF resonance frequency due to interaction with the sample surface is measured by a PLL and used as the error signal in a feedback loop to control the out-of-plane motion of the translation stage carrying the sample.

There are several advantages of using a QTF as a force sensor compared to other AFM sensors. The complexity of the AFM force sensing hardware is dramatically reduced, as a QTF can be both electrically excited and detected. Quartz oscillators have high frequency stability at room temperature and low heat dissipation which is one of the reasons why QTF sensors are often used in low temperature AFMs and room temperature metrological AFM applications. In an ambient environment, the quality factor (*Q*) that describes the width of the QTF resonance is typically a few orders of magnitude higher than that of other mechanical resonators, such as cantilevers, that are commonly used as AFM sensors. The spring constant of a

QTF is much higher than the typical spring constant of a cantilever, thereby reducing jump-to-contact problems.

The nominal resonance frequency of a QTF depends on its geometry and on the mechanical and piezoelectric properties of the quartz from which it was fabricated. The QTFs used here have a nominal resonance frequency of 32 768 Hz. A typical resonance curve of a bare QTF is shown in Fig. 3 (black line). The measured resonance frequency f_0 is slightly lower (f_0=32 765 Hz) than the nominal value (32 768 Hz). In a similar fashion, we have measured the resonance response of a QTF with a tip mounted on one of the tines and deduced the corresponding electronic parameters and the quality factor by fitting the equivalent RLC circuit model [10] (red line in Fig. 3) to the measured resonance curve (circles). The values of the electrical QTF parameters determined from the fit are also given in Figure 3.

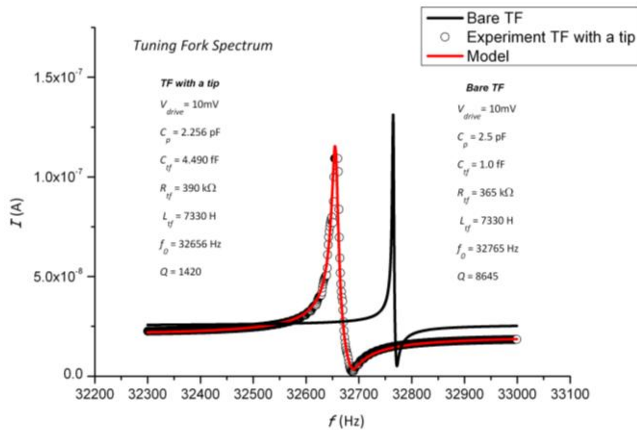

Figure 3: Measured (circles) and modeled (red line) resonance curve of a QTF with an AFM tip attached to one of the tines. The resonance curve for a bare QTF is shown by the black line. Also listed are the QTF electrical parameters.

3 ENVIROMENTAL CONTROL

In designing the instrument, special attention has been paid to minimizing the influence of environmental disturbances such as electronic and acoustic noise, vibrations and temperature fluctuations. In addition to the high symmetry and compactness of the metrological frame, this is achieved by employing low-thermal expansion materials such as super-invar, for the metrological frame. The instrument is operated in a laboratory where environmental conditions such as temperature and humidity are tightly controlled. Additional control of environmental parameters such as temperature, atmosphere and ambient vibrations is achieved by placing the mSPM structure in a chamber that allows operation in vacuum, controlled gas atmospheres, or air. The microscope and the beam delivery optics are mounted on a vibration isolation table which in turn rests on a pillar that is seismically decoupled from the building floor. The table is surrounded by a thermal enclosure which is flushed with thermalized, highly filtered air. The most significant heat source, the laser head, is spatially separated from the instrument by operating it in another room. Multiple temperature sensors and resistive heaters are embedded in the mSPM body to allow for the detection and active compensation of residual thermal gradients.

Typical peak-to-peak variations of the ambient temperature in the laboratory are 100 mK/day; in the instrument body, these reduce to about 10 mK/day. Sub-nm stability of the interferometry over several hours of operation has been demonstrated, as shown in Figure 4.

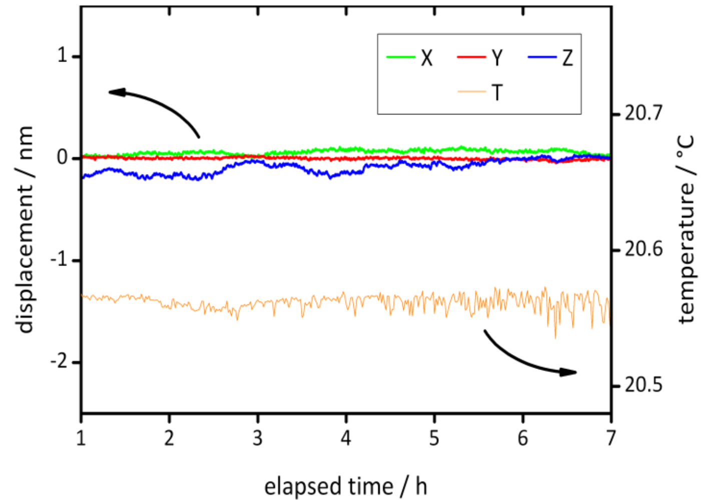

Figure 4: Simultaneous measurement of the displacement signals from the three interferometers oriented along the axes of the translation stage (X, Y, and Z, respectively) and of the temperature in the laboratory (T).

4 FREQUENCY MODULATED AFM IMAGING

The mSPM is operated in FM AFM mode where changes in the tip-sample interaction are monitored, using a PLL, via the associated shift in the QTF resonance frequency [11–13].

Preliminary images have been acquired in FM AFM mode achieving truly non-contact imaging of the sample surface. The SPM imaging is performed in a feedback loop, where the typical frequency error signal is below 1 Hz. Fine tuning of the control parameters is necessary to achieve optimal imaging in FM AFM mode. A typical SPM image of a two-dimensional (2D)-grid artifact acquired with a relatively slow scan rate (0.2 Hz) under standard laboratory conditions, i.e., outside of the environmental enclosure, is shown in Figure 5. The achieved Z resolution of the mSPM is below 1 nm. The following FM AFM parameters were used in acquiring the image: amplitude A = 89 nm, drive frequency f_0 = 32 565 Hz, frequency shift set point Δf = -17.3 Hz.

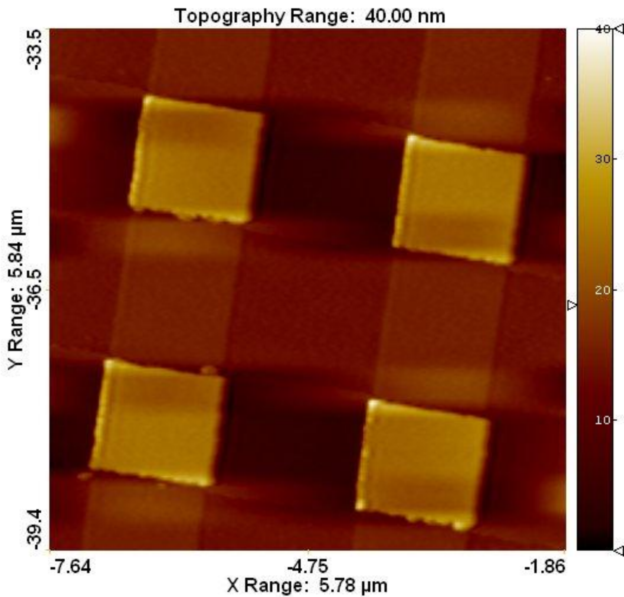

Figure 5: mSPM image of a 2D-grid artifact taken in FM AFM mode.

5 CONCLUSION

The design, manufacture and assembly of an mSPM at NMIA has been completed, and commissioning is underway. The mSPM is the key instrument in NMIA's SPM metrology facility, traceably linking dimensional measurements at the nanoscale with the realization of the SI definition of the metre at NMIA. This traceability will be achieved by measuring the displacement of the sample translation stage interferometrically in three dimensions using a frequency stabilized laser which can be calibrated against NMIA's realisation of the SI metre. The mSPM incorporates a quartz tuning fork oscillator as a non-contact force probe, a flexure-hinged, piezo-actuated three axis translation stage, and a plane mirror differential heterodyne interferometry system. To achieve the target combined uncertainty of 1 nm, the mSPM is designed to minimise uncertainties caused by thermal expansion and distortion, alignment errors and environmental vibration.

The primary application of the mSPM is to calibrate transfer standard artifacts, thereby providing traceability to the SI metre for nanoscale dimensional measurements made with instruments such as SPMs and electron microscopes. In addition, it provides a measurement capability for traceable dimensional measurements of nanomaterials such as nanoparticles.

REFERENCES

[1] S. T. Smith and D. G. Chetwynd, "Foundations of ultraprecision mechanism design", Gordon and Breach, Amsterdam, 1998.

[2] G. Wilkening, and L. Koenders, Eds, "Nanoscale calibration standards and methods", Wiley-VCH, Weinheim, 2005.

[3] H. U. Danzebrink, L. Koenders, G. Wilkening, A. Yacoot, and H. Kunzmann, "Advances in scanning force microscopy for dimensional metrology", CIRP Annals-Manufact. Technol., vol. 55, pp. 841–878, 2006.

[4] V. Korpelainen, J. Seppä, J., and A. Lassila, "Design and characterization of MIKES metrological atomic force microscope", Precis. Engineering, vol. 34, pp. 735–744, 2010.

[5] J. A. Kramar, R. Dixson, and N. G. Orji, "Scanning probe microscope dimensional metrology at NIST", Meas. Sci. Technol., vol. 22, pp. 024001–024011, 2011.

[6] R. Koning, J. Flugge, and H. Bosse, "A method for *in situ* determination of Abbé errors and their correction", Meas. Sci. Technol., vol. 18, pp. 476–481, 2007.

[7] T. G. McRae, M. T. L. Hsu, C. H. Freund, D. A. Shaddock, J. Herrmann, and M. B. Gray, Opt. Lett. 35, 2448–2450 (2012).

[8] M. T. L. Hsu, I. C. M. Littler, D. A. Shaddock, J. Herrmann, R. B. Warrington and M. B. Gray, Opt. Lett. 35, 4202 (2010).

[9] F. J. Giessibl, "Advances in atomic force microscopy", Rev. Mod. Phys., vol. 75, pp. 949–983, 2003.

[10] Y. Qin and R. Reifenberger, "Calibrating a tuning fork for use as a scanning probe microscope force sensor", Rev. Sci. Instrum., vol. 78, p. 063704, 2007.

[11] S. F. Jacobs, C. Johnston, and D. E. Schwab, "Dimensional instability of Invars", Appl. Opt., vol. 23, pp. 3500–3502, 1984.

[12] J. W. Berthold III, S. F. Jacobs, and M. A. Norton, "Dimensional stability of silica, Invar, and several ultralow-thermal expansion materials", Metrologia vol. 13, pp. 9–16, 1977.

[13] F. J. Giessibl, S. Hembacher, H. Bielefeldt, and J. Mannhart, "Subatomic features on the silicon (111)-(7×7) surface observed by atomic force microscopy", Science, vol. 289, pp. 422–425, 2000.